

A plan template based automation solution for optimization using a commercial treatment planning system

Xiaotian Huang¹, Bo Zhao², Wing Zhou³, Yan Chen³, and Hong Quan^{1*}

1.School of Physics and Technology, Wuhan University

2.Department of Radiation Oncology, Peking University First Hospital, Beijing, China and

3.Elekta (Shanghai) Instruments Ltd, Beijing, China

(Dated: November 3, 2018)

Purpose: To develop an automation platform for generating clinically acceptable plans using a commercial treatment planning system (TPS).

Methods: Unmanned planning trials on the Elekta Monaco TPS were performed with updated constraints, which were managed by the template that controls all input parameters for optimization. A software tool called Robot Framework was used to interface with Monaco to launch a plan trial. The resulting plan was evaluated in order to identify the plan quality indices that failed to meet the acceptance criteria in the prescription. Plan evaluation results, along with certain optimization parameters in Monaco, such as organ-at-risk constraints conflicting with target coverage and their achieved values, as well as adaptively adjusted relative weightings, were used to as the input to a template modifier to derive the new constraint values for the next trial. The template modifier, developed in Python, mimicked the thinking process of an experienced planner to search for the optimal strategy of optimizing a treatment plan. Acceptable plans, as with all prescribed constraints satisfied, were saved for further evaluation by clinicians. The feasibility of our automated planning approach was validated by 10 prostate and 10 Head&Neck treatment planning cases.

Results: For prostate and Head&Neck VMAT cases, auto plans were very similar to the clinical plans in terms of dose-volume histogram criteria. Some of OARs dose sparing including parotids in auto plans are significantly better than clinical ones. However, much more hot spots all appeared in these auto plans. Acceptable plans could be generated by less than 30 trials for fluence optimization only, and the quality of final plans were weakly dependent of the parameters in the starter template and the choices of the step sizes for changing the dosimetric constraint values.

Conclusion: A planning automation solution facilitated by the template in Monaco has been developed that will potentially replace the lengthy process of planner-TPS interactions.

Keywords: Monaco TPS, Template, Radiotherapy, VMAT.

* Author to whom correspondence should be addressed. Electronic mail: csp6606@sina.com

I. INTRODUCTION

With tremendous flourish of machine learning and big data, radiation therapy has been targeted as a main application of these automation technologies [1]-[2], by all kinds of tools like Keras, Torch, Tensorflow [3] launched by google on various deep learning platforms. In terms of radiation oncology, machine learning especially deep learning has profoundly been applied to realize the automation of whole radiation therapy workflow such as auto-segmentation [4], auto-planning [5], auto-QA and even pseudo-CT generation [6] by deep learning for MRI only treatment planning in the adaptive radiotherapy etc.

Auto treatment planning in radiotherapy has already been widely investigated as approximately 100 related papers were published in last years. It intends to assistant planners to generate more plans in the same time and fully ensure the consistency of plan qualities. Recently, many scholars have already explored different methods in auto-planning from knowledge-based to learning-based model. Actually, several vendors have already launched the commercial scripts based on their TPS to facilitate the original inefficient workflow of treatment plan design. Current auto-planning technology mainly focus on scripts control combined with dose prediction as the prior knowledge of rational dose distribution. Wang [5]-[7] proposed an autopilot scheme to mimic the process of IMRT/VMAT planning via scripts to records the interactions between planners and TPS, to harness the prior information like step size adjustments of dosimetric parameters in each optimization, fully improve the treatment planning efficiency. However, this approach was so inflexible that nearly all the adjusting steps was fixed. Also, to make the system more intelligent and flexible, Yan [8]-[9] has introduced an AI-guided parameters optimization (weighing factors, dose specification and dose prescription) method to achieve the automation of inverse planning and clinical application of this fuzzy inference system [10] in specific case has been accomplished. Moreover, based on the FIS, an advanced adaptive neuro fuzzy inference system (ANFIS) raised by Stieler [11] increase the learning capability of the system and use the prior data more efficiently when optimizing parameters of a complicated treatment plan. Yet, in Monaco TPS, Breedveld [12] proposed a multi-criteria optimization of beam angles called iCycle, where intensity modulated radiotherapy(IMRT) profiles in template can find a Pareto optimal plan in an acceptable time. This method mainly focused on the data collection and model buildup on the commercial TPS platform while the limitation of model generalization with big data was still an obstacle of these technology development. To solve these problems, the setup of data base can also be a solution to these kind of technologies. Thus, Fan [11] use the kernel density estimation [13] method, combined with dataset optimization, to devise an auto-planning workflow, which improve the quality and consistency of breast and rectum treatment plan. Also, Boylan [14] has compared seven beam IMRT and dual Arc VMAT technologies via scripts from data base. More and more clinical experiments via iCycle also been testified by Buergy [15], Haveren [16], which reduce the time wasted in trial-and-error adjustments of parameters in template and improved the generalization of model itself.

As Winkel[17] listed the whole optimization calculation procedure in Monaco TPS (Elekta AB) consists of two stages: fluence map optimization and segmentation optimization. In Monaco TPS, a good template could tremendously improve the planning efficiency while generation of an optimal template costs a lot time and human labors. So to utilizing computer to searching for a good template seems to be a feasible road to treatment planning. Essentially, modification of isoconstraints, isoeffects, weights during optimizing a treatment plan is equivalent to the change of a plan template. To find an expected dose distribution in fluence map optimization was of great benefit to the final results. In addition, from the experts' experience, the selection of initial templates also matters a lot because a reasonable starting point was capable of facilitating the whole optimization process.

Thus, this work has three purposes: First, develop an auto-planning platform based on the prior patient data to automatically find a rational initial template as a starting point. Second, based on the platform, utilize template modifier program, combined with an evaluation system, to automatically search for an clinically acceptable plan in fluence optimization and improve the plan quality and efficiency in treatment planning. Third is to devise an extendible API for future reinforcement learning (RL) to alleviate issues of lacking enough high-quality data and make the platform more intelligent. Based on treatment plan templates, a newly auto-planning platform of parameters optimization in Monaco has been developed via the program-TPS interactions instead of planner-TPS. Combined with the new DVH statistics evaluation tool in Monaco 5.4 TPS(Elekta AB), the prescription request was used as a primary criteria for plan evaluation. In addition, as a secondary criteria, an expert's requirment was a reference to ensure the optimized treatment plan was clinical acceptable and can be delivered safely in the condition of maximizing tumor control and minimizing OARs dose sparing.

II. MATERIALS AND METHODS

A. Retrospective Planning study

10 prostate cases and 10 SIB(simultaneous-integrated boost) head&neck cases were selected to testify the feasibility of this research. Those patients were treated with 6MV Elekta Synergy at Peking Univeristy First Hospital from June 2016 to Decemeber 2017. All the VMAT treatment plans were manually created by 2 dosimetrists using Monaco 5.11 TPS (Elekta AB). TableIII and TableIV in supplementary materials gives the detailed prescription information. To make a reliable comparison,the auto plans have the same dosimetric criteria with clinical ones and all the sequencing settings and dosimetric parameters were kept the same between clinical and auto planning.We compared the clinical plans and auto plans with a two-sided Wilcoxon signed-rank test to assess statistical significance ($p < 0.05$).

B. Sensitivity Analysis

Adjusting constraints in case the target dose does not meet the expectation can be very cumbersome if no additional information is provided. The sensitivity analysis can provide the conflicts between goals and constraints, which help planners avoid fruitless trial. But it is not easy to teach our program to recognize and understand the meaning of sensitivity. In this work, inspired by Alber's idea [18] of sensitivity analysis of optimization, we tried to quantify the sensitivity information to assist template modifier program automatically search the solution more informatively. In addition, given sensitivity actually was the language multipliers reflecting differential information in constrained optimization in Monaco TPS, which was used to balance the gradient of objective function and constraints,so we explored the specific numerical relationship between updated isoconstraint and sensitivity, isoeffects to make more accurate modification of these parameters in template. Fig. 1 shows the sensitivity window in Monaco. Equation1 demonstrates a part of Karush-Kuhn-Tucker condition in optimization when gradients of language function is zero. f and g indicate the objective and constraint functions with respect to voxel dose $D(\phi)$ and weight ϕ . λ_i was the language multiplier, which also reflects the sensitivty in Monaco TPS(Elekta AB). More details could be founded in [19].

$$\nabla_{\phi} f^* = - \sum_{i=1}^m \lambda_i^* \nabla_{\phi} g_i \quad (1)$$

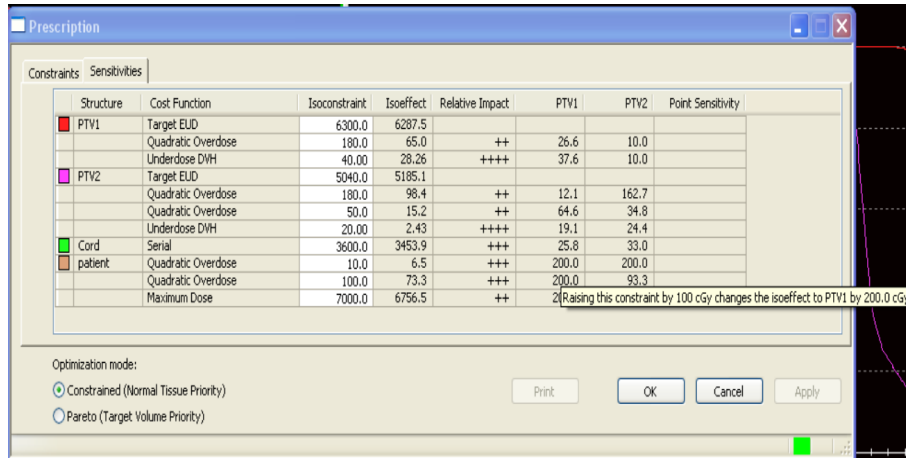


FIG. 1: The sensitivity window in Monaco (Conflicts between constraints and goals)

C. Auto-planning platform

Here, we developed an auto-planning platform, displayed in Fig. 2, which replaced human to interface with Monaco TPS (Elekta AB). This platform can mimic planners thinking process to manipulate the TPS and make clinical treatment plan. Following are the main four parts of this platform.

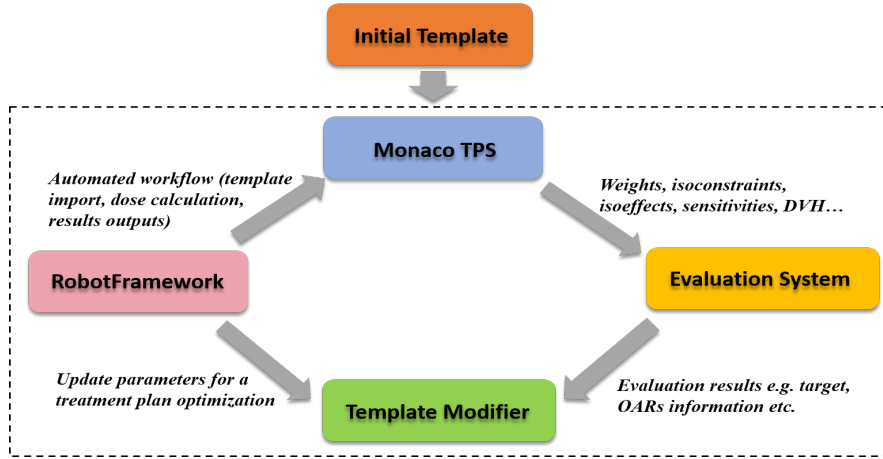


FIG. 2: The auto-planning platform

1. Robotframework

RobotFramework(RIDE), as seen in Fig. 2 and Fig. 3, is harnessed to automatically control TPS. Analogous to scripts, this application can realize each manipulation of TPS such as new treatment plan trial, saving dosimetric parameters, adjust beam angles through inner written keywords. Thus, a clinical treatment planning process can be split into several steps and each step can be written as a keyword to automatize the planning workflow. In this work, as a control system, RIDE has three functions: 1) automatically load a new plan template; 2) automatically execute fluence optimization; 3) automatically export the dose-volume histogram results.

\$(iter)	Config Read	\$(iteration)	iteration	iteration	
: FOR	\$(index)	IN RANGE	0	\$(iter)	
	comment	Check flag			
	\$(flag)	Config Read	\$(flag_pk_pros)	flag	flag
	Run Keyword If	\$(flag) == 1	log	equal 1	
	comment	Import Template			
	\$(template_hh)	Config Read	\$(temp_pk_pros)	template	template
	\$(plan_name)	Config Read	\$(plan_pk_pros)	name	name
	\$(dvh_name)	Config Read	\$(dvh_pk_pros)	dvh_name	dvh_name
	Ribbon Toolbar Click Item	tabPlanning			
	Open New Monaco Plan				
	New Monaco Plan Enter Value	editPlanName	\$(plan_name)		
	New Monaco Plan Select Value	cbDelivery	VMAT		
	New Monaco Plan Select Template To Import Click Item	RTG0815prostate1			
	New Monaco Plan Close				
	Warning Dialog Click Item	btnYes			
	Map Structures Skip Mapping				
	comment	First dose calculation step			
	Optimization Start	KeepMessage			
	Warning Dialog Verify	stcWarningMessage	Value	Contains	Full Fluence Modulation Complete.
	Warning Dialog Accept				
	comment	Export DVH			

FIG. 3: Capture of Robot Framework

2. Evaluation System

Inspired by Venture[20], we used the spiderplot here, shown in Fig. 4, as the standard evaluation tool to reflect the plan's DVH indices change and illustrate a vivid trend of dose statistical change in each iteration. But as is

known to all, a plan's quality is highly dependent on the patient anatomy, especially the distance between target and OARs indicated by Zhu[21]. Also, institutional variation may cause the same plan probably has different scoring levels and criteria. However, to simplify the whole problem, each prescription of clinical cases was used as the ground truth of evaluation in this work. Evaluation system has two functions: 1) evaluate each iteration's DVH statistical results to measure difference from prescription; 2) provide template modifier with the quantitative relationship between isoconstraints, isoeffect and sensitivity.

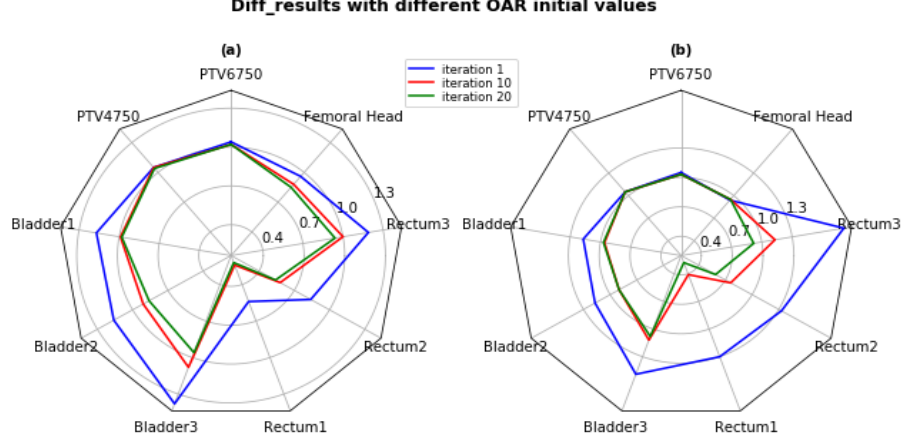


FIG. 4: Spiderplot of different initial OARs values (a, b) for plan evaluation in automated planning system.

$$(Index(PTV) = \frac{actual_target}{prescription_target}); Index(OARs) = \frac{actual_OARs}{prescription_OARs})$$

3. Template Modifier

Essentially, the treatment planning process can be considered as an optimal strategy problem, especially in modification of dosimetric parameters like isoconstraints, isoeffects. In Monaco TPS (Elekta AB), each treatment planning trial can be driven by template because all the dosimetric related information are stored in this file(.hyp). Thus, template modifier, the core of the whole platform as depicted in Fig.2, was developed in Python(Python 3.6) to automatically update the parameters in template through an in-house devised strategy. All searching strategy was priorly written in this Modifier, driven by the plan evaluation results and Monaco optimization parameters, such as how an organ-at-risk constraint impacted target dose coverage and adaptively adjusted relative weightings of the constraints.

In this work, searching strategy can be divided into three stages: first two steps were used to optimize the target coverage through adjusting the shrink margins and "Patient" cost function in Monaco TPS(Elekta AB). If the target coverage is satisfied well, then third step was executed, which was capable to constrain some OARs, conflicting with target. The flowchart of this strategy in template modifier is shown in Fig. 5 and details of third steps is depicted in Fig. 6. The maximum iteration number for each stage are set to 15, 15 and 30 respectively, which means if the searching time exceed the setting ones, the program will stop. All plan optimization progress in Monaco TPS (Elekta AB) was considered as a blackbox and each iteration include the import/export of the treatment plan, parameters updating, plan evaluation.

4. Template Initialization

Here, we also innovatively developed a template generator in Python, based on the experts' experience as a prior information, to generate a suitable plan template automatically as an initial value in later optimization and Fig. 7 shows the detailed flowcharts. Once the prescription files(.csv) and contoured structure files(.dcm) were prepared, according to the template set stored before, a initial plan template including prescription dose, cost functions, optimization constraints, grid selection, delivery approach was generated automatically by the template generator

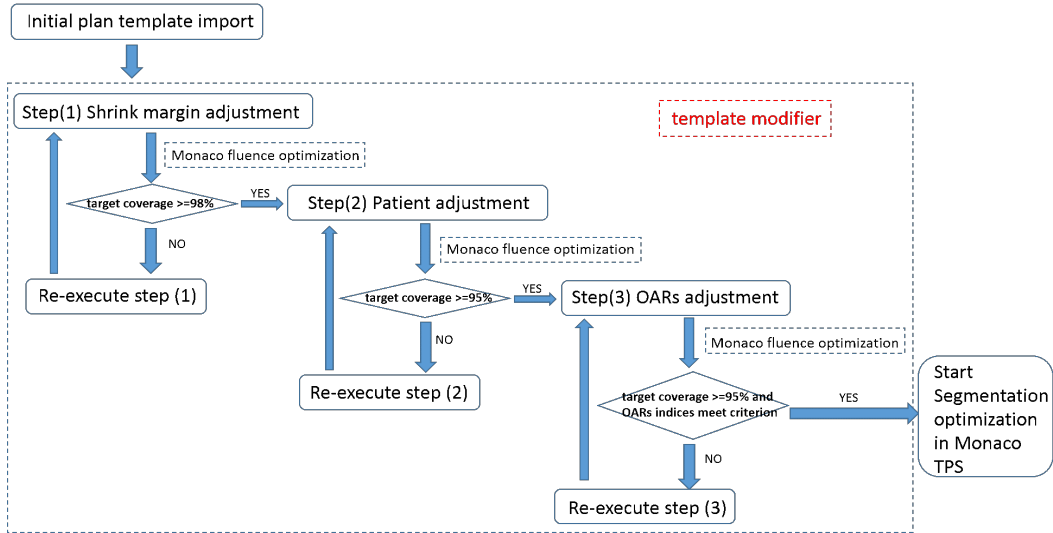


FIG. 5: Display of the detailed flowcharts in the template modifier.

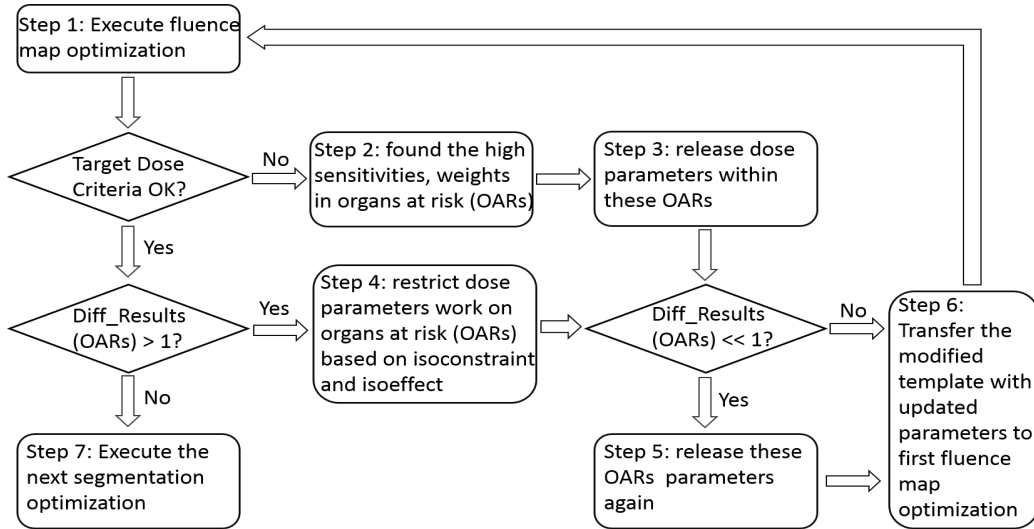


FIG. 6: Illustration of details in third step.

program. Our experimnts in prostate cases and H&N cases indicates if the initial template was suitable and results in fluence optimization all meets the prescription, segmentation optimization can be executed directly and the final results were mostly acceptable.

D. VMAT treatment planning execution

In this auto-planning platform, one iteration includes plan initialization, dose calculation and optimization, output DVH(Dose Volume Histogram), plan evaluation. Fig. 8 displays the estimated time consumption in one iteration. To improve the calculation efficiency, in each iteration only fluence map optimization was executed. All the optimization parameters such as isoconstraints, isoeffects, weights and sensitivity can all stored to be used for guiding the modification of template in next iteration.

Before execution of whole optimization loop, structure name and order variation should be carefully considered. In Monaco TPS(Elekta AB), we need to check if the structure name in template is consistent with the TPS to avoid the name mismatch, which may cause malfunction of the TPS. In additin, order variation of each structure and its

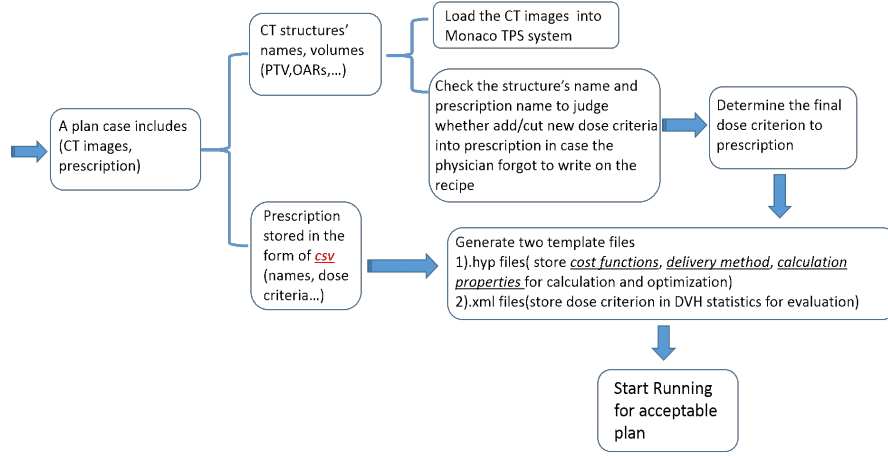


FIG. 7: Demonstration of the initial plan template file generation based prior information

cost functions set in Monaco could also influence the final results. So in our experiments, to ensure the consistency, it's indispensable to select a fixed and rational structure sequence in template. Experiments were all carried in a workstation equipped with two Intel(R) Xeon(R) 2.5 GHz processors (48 cores) and 48 GB RAM.

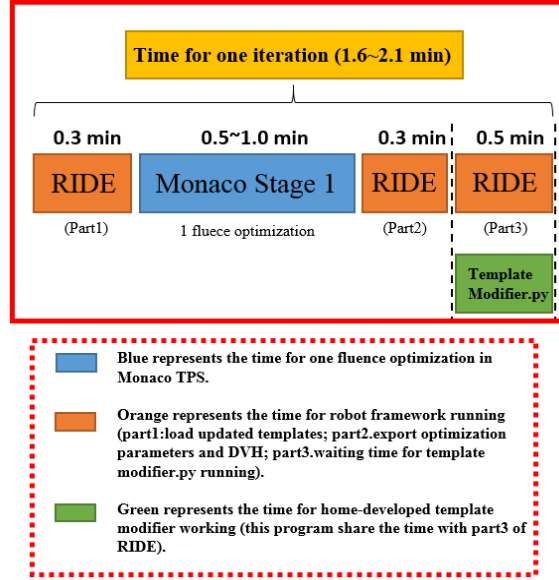


FIG. 8: The time cost for one iteration in the whole autoplanning workflow.

III. RESULTS

A. Prostate VMAT cases

Fig. 9 depicts the side-by-side isodose comparison between clinical plan and auto plan. Actually, the target dose coverage and the isodose distribution are very similar between clinical and auto plan. In addition, compared to clinical plans, there are much less overlaps of bladder and low dose region (pink line) shown in auto plan, which means more dose sparing of OARs. DVH statistics indices change of target and OARs in 40 iterations is also displayed in Fig. 10(a). It's obvious that after 15-20 iterations, all the OARs' metrics are converged while PTV6750 seems still oscillating all the time, which mainly due to the dose reset in each fluence optimization. Moreover, step size variation seems

no impact on the optimization process. Fig. 10(b) illustrates the DVH shape change, where dose in bladder can be apparently controlled well.

Fig. 11 shows the final results of DVH and nearly tiny discrepancy of PTV6750 between clinical and auto plan could be found. In auto plan, PTV4750 and rectum dose increased a little bit while dose in bladder is reduced dramatically. The detailed mean DVH statistics indices difference were listed in Table I. There is no significant difference between clinical plans and auto plans except the maximum dose in auto plans, which is approximate 1Gy higher than clinical ones.

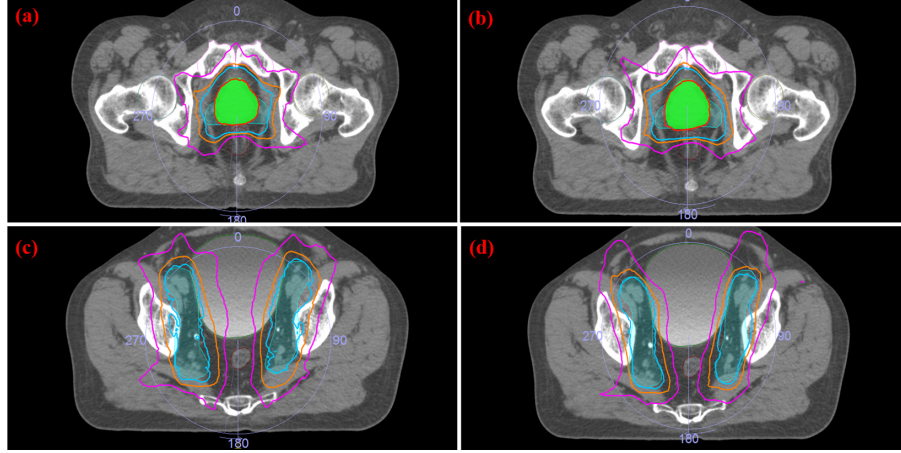


FIG. 9: Side-by-side dose distribution comparison of automated (b,d) and clinical (a,c) prostate planning.

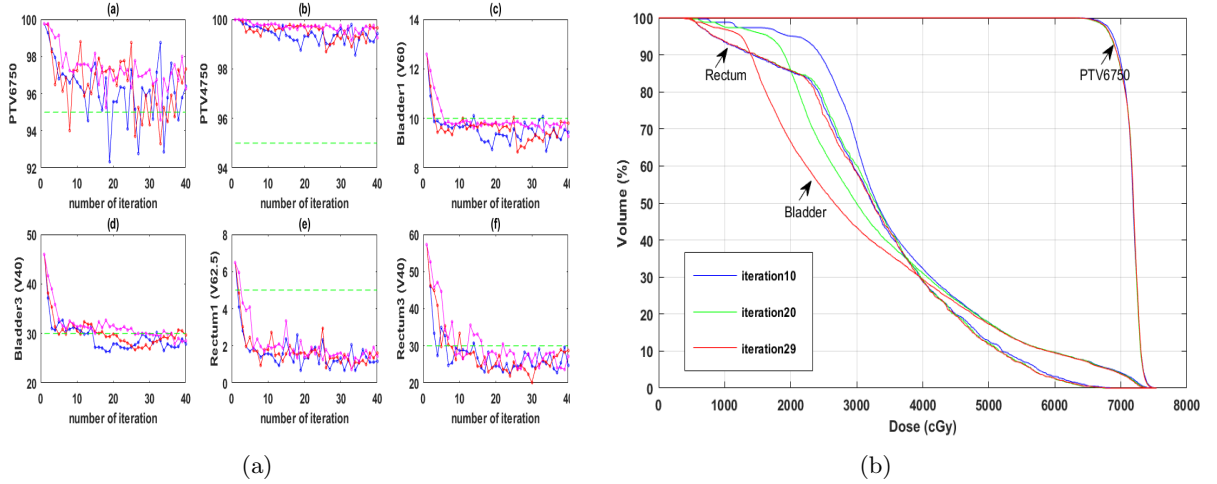


FIG. 10: (a) Three different step size comparison of dose-volume histogram indexes changes. Dot green line is prescription request, step size (blue line) > step size (red line) > step size (magenta line);(b) DVH shape alterations in different iterations (10, 20, 29).

In 10 prostate prostate cases, to simplify the workflow, we first automatically generated the initial plan template files with our own program and then transfer them into Monaco TPS (Elekta AB) automatically. The average optimization time include template modification for fluence optimization is about 15-30 min within 15 iterations. In this procedure, we priorly set the maximum iterations for breaking out. We found some cases can directly do segmentation optimization after 1-2 fluence optimization if the case is not so complicated. However, in some cases, if PTV overlays too many Bladder or Rectum, the optimization time in each iteration last longer.

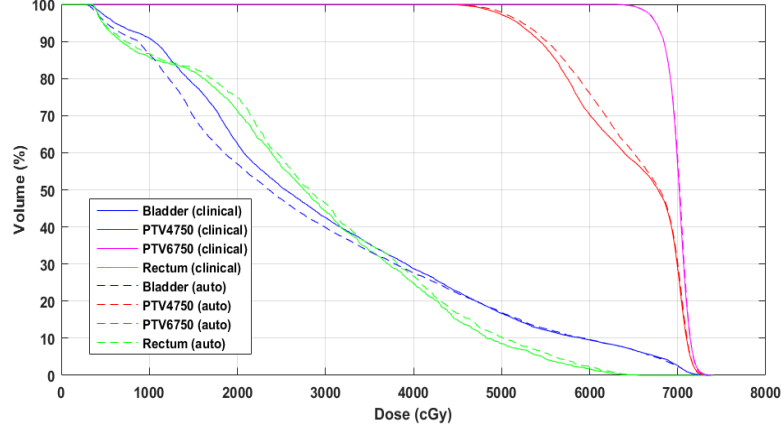


FIG. 11: Final dose-volume histogram comparison of dose distributions between auto prostate planning and clinical planning.

TABLE I: 10 prostate cases DVH statistics

Prescription	Clinical(mean \pm std)	Auto(mean \pm std)	P value
PTV6750(V67.5Gy \geq 95%)	96.23 \pm 1.72	95.74 \pm 1.54	0.799
PTV4750(V47.5Gy \geq 95%)	96.04 \pm 1.34	96.18 \pm 1.02	0.922
Bladder1(V60Gy \leq 10%)	6.88 \pm 6.40	6.08 \pm 4.30	0.721
Bladder2(V50Gy \leq 20%)	11.5 \pm 9.30	11.51 \pm 7.78	0.375
Bladder3(V40Gy \leq 30%)	25.22 \pm 9.18	24.20 \pm 9.40	0.432
Rectum1(V62.5Gy \leq 5%)	3.03 \pm 2.14	2.84 \pm 2.85	0.625
Rectum2(V50Gy \leq 20%)	13.45 \pm 4.09	12.48 \pm 5.68	0.77
Rectum3(V40Gy \leq 30%)	26.42 \pm 5.78	26.89 \pm 8.60	0.234
Pubic Bone(V62.5Gy \leq 15%)	7.17 \pm 5.08	4.76 \pm 4.82	0.124
Femoral Head L(Dmax \leq 54Gy)	42.75 \pm 4.64	41.61 \pm 4.85	0.557
Femoral Head R(Dmax \leq 54Gy)	41.91 \pm 4.77	42.36 \pm 5.64	0.695
Maximum Dose(Dmax \leq 74.25Gy)	73.07 \pm 1.11	74.27 \pm 0.73	0.027

B. Head&Neck VMAT cases

Side-by-side final isodose comparison is demonstrated in Fig. 12. Low dose region in auto-plan is relatively smaller than clinical plan. The dose sparing of parotids and brain stem in auto plan are also much better than clinical plan. However, in auto plan if too much constraints work on the OARs, the appearance of hot spot may influence the homogeneity of the plan. Fig. 13 (a) depicts the DVH indices changing process in 30 iterations. Nearly all the OARs(organs at risk) dose converge in short time. In the meanwhile, target coverage is maintained very well. To improve the flexibility of program, the step size settings in template modifier were adaptive controlled by the dose optimization parameters like sensitivity, isoeffects, etc. Fig. 13 (b) gives spiderplot of DVH indices change in the head&neck. All the indices was normlized by prescriprion. The coverage tendency is consistent with plot (a). Fig. 14 displays the final DVH comparison, in which only the spinal cord dose reduced tremendously. The detailed statistics information of H&N are also listed on Table II. Most Statistics Indices including target coverage has no significant difference except spinal cord, parotids, mandible and maximum dose.

After the prescription and structure were given, the template generator could provide 2-3 plan templates as candidates for fluence optimization. Through some trials, results indicate some templates were not flexible in cost function selection so the most suitable ones should be set as the initial template for template modification in fluence optimization. When optimizing the H&N cases, much more optimization time, about 20-30 iterations, would be cost mainly due to the complication of the cases.

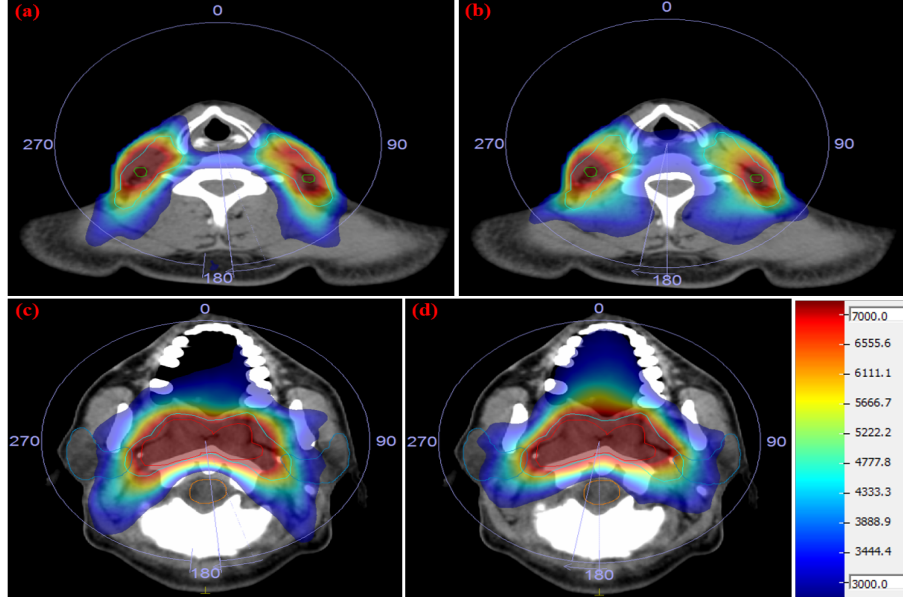


FIG. 12: Comparison of the isodose distribution of automated (a,c) and clinical (b,d) head&neck planning.

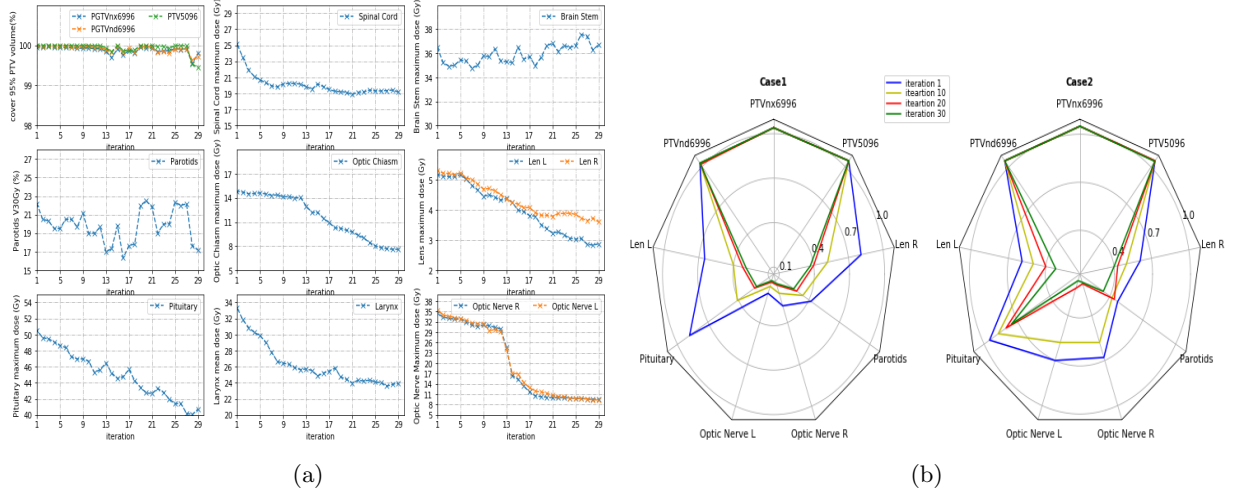


FIG. 13: (a) This plot indicates the OARs and target indices change of head&neck cases in 30 iterations. (b) Spiderplot of head&neck cases to depict the change of DVH indices.

IV. DISCUSSION

The main innovation of this study is the proposition of a new template based auto-planning platform mainly composed of template generator, template modifier, evaluation system. This platform can automatically generate initial treatment planning template and automatically search for a clinical optimal template based on prior planners' experience, improving the planning efficiency and ensuring the consistency and quality of our clinical treatment plan.

Breedveld [22] have already developed the iCycle, a multi-criterial and orientation optimization platform based on wish-list of template, to optimize a treatment plan on Monaco TPS and the final output is an optimal template. Although several researches [23][15][24] of iCycle show the auto-planning preforms better than clinical plan not only in efficiency but also in reduction of dose on critical structures, the whole process was isolated from Monaco TPS, which may still need manual modification of template when the final dosimetric results like DVH(Dose Volume Histogram) are unacceptable. Our platform can be relatively more flexible to modify the template timely if the final results are unsatisfied. Wang [7] also build up a script-based auto-planning based on commercial TPS while it lacks consideration of some important geometric and physical factors, which may influence the final results. In addition,

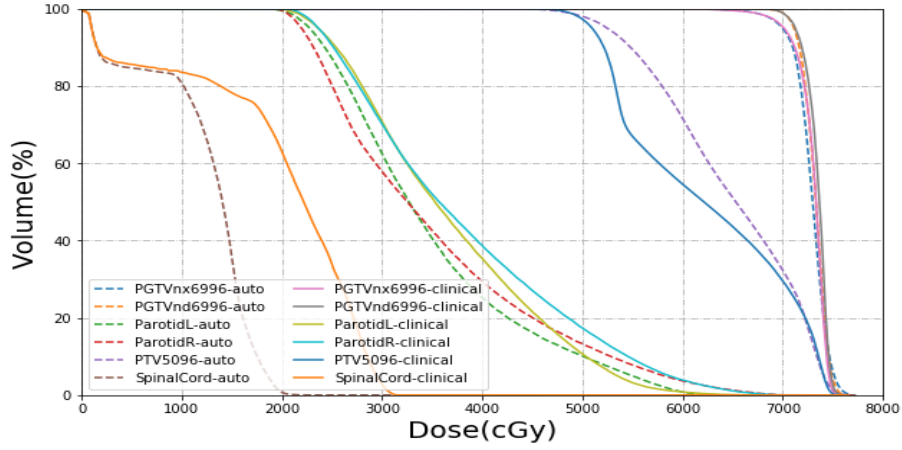


FIG. 14: Final DVH comparison between auto and clinical head&neck planning.

TABLE II: 10 Head&Neck cases DVH statistics

Prescription	Clinical(mean \pm std)	Auto(mean \pm std)	P value
PTVnx6996(V69.96Gy \geq 95%)	96.92 \pm 1.21	96.02 \pm 1.57	0.341
PTVnd6996(V69.96y \geq 95%)	98.02 \pm 1.30	97.01 \pm 1.80	0.084
PTV5096(V50.96Gy \geq 95%)	97.53 \pm 1.79	96.26 \pm 1.49	0.097
Brain Stem(Dmax \leq 54Gy)	45.85 \pm 4.47	42.23 \pm 5.09	0.160
Spinal Cord(Dmax \leq 40Gy)	33.63 \pm 1.53	28.48 \pm 4.87	0.027
Left Len(Dmax \leq 9Gy)	3.05 \pm 1.98	3.78 \pm 2.29	0.027
Right Len(Dmax \leq 9Gy)	3.23 \pm 1.72	3.73 \pm 1.98	0.160
Left Optic Nerve(Dmax \leq 54Gy)	18.96 \pm 17.10	19.28 \pm 18.09	0.846
Right Optic Nerve(Dmax \leq 54Gy)	23.11 \pm 17.27	19.36 \pm 18.27	0.492
Optic Chiasm(Dmax \leq 54Gy)	21.50 \pm 16.88	22.77 \pm 18.68	0.625
Parotids(V50Gy \leq 30%)	29.03 \pm 10.98	26.96 \pm 8.58	0.0039
Esophagus(Dmean \leq 40Gy)	29.74 \pm 5.19	31.21 \pm 6.03	0.322
Mandible(Dmean \leq 50Gy)	38.54 \pm 4.68	34.98 \pm 4.19	0.010
Maximum Dose \leq 76.95Gy	76.45 \pm 0.62	77.89 \pm 1.24	0.010

the searching strategy is fixed for optimizing, which may not suitable for more clinical cases.

In this study, much higher the maximum dose in both auto prostate and head&neck cases indicated that our system is still incapable of controlling hot spot in target volume mainly due to the OARs too exacting constraints, which may sacrifice parts of target dose coverage at the same time decreased dose distribution heterogeneity in target volume. However, on account of limited patient data, more clinical trials should need to be tested to verify this effect.

Frankly, all the automation implemented on the Stage1(flucence optimization) would cause the results inconsistency between Stage1 and Stage2(MC) due to the variation of dose calculation algorithm, which may results in an unpredictable final dose distribution optimized from Stage2. However, inconsistency was hardly found Fig. 15 in our experiments on prostate and H&N cases. Zheng [25] indicates the target coverage would be reduced a little from PB to MC, which is consistent with our results. He also reported the prediction of dose calculation difference between PB(pencil beam) and MC(Monte Carlo) algorithm, which could be applied to our platform in future.

Generally, in Monaco TPS(Elekta AB), the whole planning process was unable to be tracked if planners did warm start in the fluence optimization, which to some extents caused the final plan fail to be reimplemented to obtain the same results while with the help of autoplanning, all the optimization parameters like isoconstraints, isoeffect, etc, can all be tracked and stored in the defined variables for repetition. After the optimization of one plan, clinicians

DVH Statistics			DVH Statistics			DVH Statistics		
Dosimetric Criteria			Dosimetric Criteria			Dosimetric Criteria		
Structure	Dosimetric Criterion	Actual Value	Structure	Dosimetric Criterion	Actual Value	Structure	Dosimetric Criterion	Actual Value
PGTvnx6996	V6996Gy > 95 %	98.76 %	PGTvnx6996	V6996Gy > 95 %	81.61 %	PGTvnx6996	V6996Gy > 95 %	95.00 %
PGTVnd6996	V6996Gy > 95 %	98.21 %	PGTVnd6996	V6996Gy > 95 %	82.41 %	PGTVnd6996	V6996Gy > 95 %	95.91 %
PTV5096	V5096Gy > 95 %	99.74 %	PTV5096	V5096Gy > 95 %	94.08 %	PTV5096	V5096Gy > 95 %	96.28 %
Spinal Cord	Dmax < 4000 cGy	2242.7 cGy	Spinal Cord	Dmax < 4000 cGy	2177.1 cGy	Spinal Cord	Dmax < 4000 cGy	2221.3 cGy
Brain Stem	Dmax < 5400 cGy	3293.6 cGy	Brain Stem	Dmax < 5400 cGy	3499.5 cGy	Brain Stem	Dmax < 5400 cGy	3571.3 cGy
Len L	Dmax < 900 cGy	261.1 cGy	Len L	Dmax < 900 cGy	151.8 cGy	Len L	Dmax < 900 cGy	154.9 cGy
Len R	Dmax < 900 cGy	332.5 cGy	Len R	Dmax < 900 cGy	181.2 cGy	Len R	Dmax < 900 cGy	184.9 cGy
Optic Chiasm	Dmax < 5400 cGy	744.8 cGy	Optic Chiasm	Dmax < 5400 cGy	570.5 cGy	Optic Chiasm	Dmax < 5400 cGy	582.2 cGy
Optic Nerve L	Dmax < 5400 cGy	587.3 cGy	Optic Nerve L	Dmax < 5400 cGy	328.8 cGy	Optic Nerve L	Dmax < 5400 cGy	335.5 cGy
Optic Nerve R	Dmax < 5400 cGy	667.4 cGy	Optic Nerve R	Dmax < 5400 cGy	364.7 cGy	Optic Nerve R	Dmax < 5400 cGy	372.2 cGy
Pituitary	Dmax < 5400 cGy	1280.9 cGy	Pituitary	Dmax < 5400 cGy	1142.2 cGy	Pituitary	Dmax < 5400 cGy	1165.6 cGy
Inner Ears	Dmax < 5400 cGy	5335.0 cGy	Inner Ears	Dmax < 5400 cGy	5011.1 cGy	Inner Ears	Dmax < 5400 cGy	5113.9 cGy
Esophagus	Dmean < 4000 cGy	3177.6 cGy	Esophagus	Dmean < 4000 cGy	2991.3 cGy	Esophagus	Dmean < 4000 cGy	3052.7 cGy
Trachea	Dmean < 4000 cGy	2684.0 cGy	Trachea	Dmean < 4000 cGy	2373.6 cGy	Trachea	Dmean < 4000 cGy	2422.4 cGy
Thyroid	V5000cGy < 50 %	50.31 %	Thyroid	V5000cGy < 50 %	22.35 %	Thyroid	V5000cGy < 50 %	27.46 %
Mandible	Dmean < 5000 cGy	3748.7 cGy	Mandible	Dmean < 5000 cGy	3569.5 cGy	Mandible	Dmean < 5000 cGy	3642.8 cGy
Oral Cavity	Dmean < 5000 cGy	3553.8 cGy	Oral Cavity	Dmean < 5000 cGy	3477.4 cGy	Oral Cavity	Dmean < 5000 cGy	3548.8 cGy
Larynx	Dmean < 6000 cGy	3053.8 cGy	Larynx	Dmean < 6000 cGy	2885.4 cGy	Larynx	Dmean < 6000 cGy	2944.6 cGy
Neck	Dmax < 4000 cGy	7087.8 cGy	Neck	Dmax < 4000 cGy	6856.8 cGy	Neck	Dmax < 4000 cGy	6997.5 cGy

Fluence Opt

MC Opt (no rescale)

MC Opt (rescale to 95%)

FIG. 15: Comparison between fluence optimization(fluence opt), Segmentation optimization(MC opt) and Segmentation optimization(MC opt with rescale 95% dose coverage to PGTvnx6996).

can track each iteration history of the plan template and final results will be repetitively implemented. Currently, the automatic warm-start realization combined with reinforcement learning, which seems the most prospective AI approach in TPS, is under researching. Essentially, the treatment planning process can be considered as a optimal strategy problem, which is very similar to basic idea, reinforcement learning, of AlphaZero [26]. Fig. 16 illustrates the potential of application in auto planning. According to [27], deep reinforcement learnig(DRL) has already been applied to radiation adaptation in lung cancer. In future, in addition to the improvment of efficiency, the robustness and intelligence of this platform would be improved dramatically.

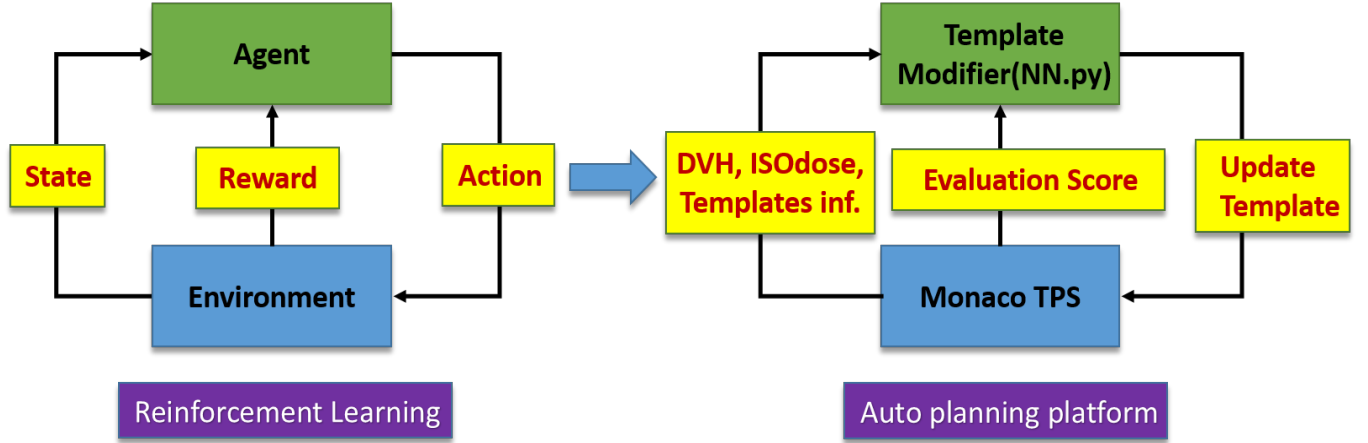


FIG. 16: The similarity between deep reinforcement learning and auto treatment planning process.

V. CONCLUSIONS

Our study have verified the feasibility of template based automation solution for VMAT/IMRT treatment planning in Monaco TPS. A auto-planning platform composed of three components: Template Modifier + Robot Framework + Evaluation System was proposed to automatize the whole treatment planning workflow as shown in Fig. 2. These three components were able to simulate the planners' thinking process and replace them interacting with TPS to optimize an acceptable plan, which tremendously facilitates the efficiency of planning workflow. However, future study need to focus on the reinforcement learning applied to this auto-planning platform, providing an more intelligent and robust solution for treatment planning.

VI. ACKNOWLEDGEMENTS

This research is technically supported by Elekta Instrument Shanghai Ltd. The author would like to thank both Elekta Instrument Shanghai Ltd for providing some of their research software tools and Charles Chen, Flora Tang, for their ongoing supports.

VII. REFERENCES

-
- [1] L. Xing, E. A. Krupinski, and J. Cai, *Medical physics* (2018).
 - [2] P. Meyer, V. Noblet, C. Mazzara, and A. Lallement, *Computers in biology and medicine* (2018).
 - [3] M. Abadi, A. Agarwal, P. Barham, E. Brevdo, Z. Chen, C. Citro, G. S. Corrado, A. Davis, J. Dean, M. Devin, S. Ghemawat, I. Goodfellow, A. Harp, G. Irving, M. Isard, Y. Jia, R. Jozefowicz, L. Kaiser, M. Kudlur, J. Levenberg, D. Mané, R. Monga, S. Moore, D. Murray, C. Olah, M. Schuster, J. Shlens, B. Steiner, I. Sutskever, K. Talwar, P. Tucker, V. Vanhoucke, V. Vasudevan, F. Viégas, O. Vinyals, P. Warden, M. Wattenberg, M. Wicke, Y. Yu, and X. Zheng, “**TensorFlow: Large-scale machine learning on heterogeneous systems,**” (2015), software available from tensorflow.org.
 - [4] K. Men, J. Dai, and Y. Li, *Medical physics* **44**, 6377 (2017).
 - [5] H. Wang and L. Xing, *Journal of applied clinical medical physics* **17**, 189 (2016).
 - [6] M. Maspero, M. H. Savenije, A. M. Dinkla, P. R. Seevinck, M. P. Intven, I. M. Jurgensliemk-Schulz, L. G. Kerkmeijer, and C. A. van den Berg, *Physics in Medicine & Biology* **63**, 185001 (2018).
 - [7] H. Wang, P. Dong, H. Liu, and L. Xing, *Medical physics* **44**, 389 (2017).
 - [8] H. Yan, F.-F. Yin, H.-q. Guan, and J. H. Kim, *Physics in Medicine & Biology* **48**, 3565 (2003).
 - [9] H. Yan, F.-F. Yin, H. Guan, and J. H. Kim, *Medical physics* **30**, 2675 (2003).
 - [10] H. Yan, F.-F. Yin, and C. Willett, *Radiotherapy and oncology* **83**, 76 (2007).
 - [11] F. Stieler, H. Yan, F. Lohr, F. Wenz, and F.-F. Yin, *Radiation Oncology* **4**, 39 (2009).
 - [12] S. Breedveld, P. R. Storchi, and B. J. Heijmen, *Physics in Medicine & Biology* **54**, 7199 (2009).
 - [13] J. S. Munter and J. Sjölund, *Physics in Medicine & Biology* **60**, 6923 (2015).
 - [14] C. Boylan and C. Rowbottom, *Journal of applied clinical medical physics* **15**, 213 (2014).
 - [15] D. Buerge, A. W. M. Sharfo, B. J. Heijmen, P. W. Voet, S. Breedveld, F. Wenz, F. Lohr, and F. Stieler, *Radiation Oncology* **12**, 33 (2017).
 - [16] R. van Haveren, S. Breedveld, M. Keijzer, P. Voet, B. Heijmen, and W. Ogryczak, *European Journal of Operational Research* **263**, 247 (2017).
 - [17] D. Winkel, G. H. Bol, B. van Asselen, J. Hes, V. Scholten, L. Kerkmeijer, and B. Raaymakers, *Physics in Medicine & Biology* **61**, 8587 (2016).
 - [18] M. Alber and R. Reemtsen, *Optimisation Methods and Software* **22**, 391 (2007).
 - [19] M. Alber, M. Birkner, and F. Nüsslin, *Physics in Medicine & Biology* **47**, N265 (2002).
 - [20] T. Ventura, M. do Carmo Lopes, B. C. Ferreira, and L. Khouri, *Reports of Practical Oncology & Radiotherapy* **21**, 508 (2016).
 - [21] X. Zhu, Y. Ge, T. Li, D. Thongphiew, F.-F. Yin, and Q. J. Wu, *Medical physics* **38**, 719 (2011).
 - [22] S. Breedveld, P. R. Storchi, P. W. Voet, and B. J. Heijmen, *Medical physics* **39**, 951 (2012).
 - [23] P. W. Voet, M. L. Dirkx, S. Breedveld, D. Fransen, P. C. Levendag, and B. J. Heijmen, *International Journal of Radiation Oncology* Biology* Physics* **85**, 866 (2013).
 - [24] M. Buschmann, A. W. M. Sharfo, J. Penninkhof, Y. Seppenwoolde, G. Goldner, D. Georg, S. Breedveld, and B. J. Heijmen, *Strahlentherapie und Onkologie* **194**, 333 (2018).
 - [25] D. Zheng, X. Zhu, Q. Zhang, X. Liang, W. Zhen, C. Lin, V. Verma, S. Wang, A. Wahl, Y. Lei, *et al.*, *Radiation Oncology* **11**, 83 (2016).
 - [26] D. Silver, J. Schrittwieser, K. Simonyan, I. Antonoglou, A. Huang, A. Guez, T. Hubert, L. Baker, M. Lai, A. Bolton, *et al.*, *Nature* **550**, 354 (2017).
 - [27] H.-H. Tseng, Y. Luo, S. Cui, J.-T. Chien, R. K. Ten Haken, and I. E. Naqa, *Medical physics* **44**, 6690 (2017).

VIII. SUPPLEMENTARY MATERIALS

TABLE III: Prescription of Prostate case

Organ Indices	Evaluation Criteria	Prescription Requests
PTV6750	Minimum Volume of PTV6750 covered by 67.5 Gy	95.0(%)
PTV4750	Minimum Volume of PTV4750 covered by 47.5 Gy	95.0(%)
Rectum1	Maximum Volume of Rectum covered by 40.0 Gy	30.0(%)
Rectum2	Maximum Volume of Rectum covered by 50.0 Gy	20.0(%)
Rectum3	Maximum Volume of Rectum covered by 62.5 Gy	5.0(%)
Bladder1	Maximum Volume of Bladder covered by 40 Gy	30.0(%)
Bladder2	Maximum Volume of Bladder covered by 50 Gy	20.0(%)
Bladder3	Maximum Volume of Bladder covered by 60 Gy	10.0(%)
Femoral Head	Maximum Dose	54.0(Gy)

TABLE IV: Prescription of the Head&Neck case

Organ Indices	Evaluation Criteria	Prescription Requests
PGTVnx6996	Minimum Volume of PTVnx6996 covered by 69.96 Gy	95.0(%)
PGTVnd6996	Minimum Volume of PTVnd6996 covered by 69.96 Gy	95.0(%)
PTV5096	Minimum Volume of PTV5096 covered by 50.96 Gy	95.0(%)
Spinal Cord	Maximum Dose	40.0(Gy)
Cord PRV	Maximum Dose	45.0(Gy)
Brain Stem	Maximum Dose	54.0(Gy)
Stem PRV	Maximum Dose	60.0(Gy)
Len L	Maximum Dose	9.0(Gy)
Len R	Maximum Dose	9.0(Gy)
Optic Chiasm	Maximum Dose	54.0(Gy)
Optic Nerve L	Maximum Dose	54.0(Gy)
Optic Nerve R	Maximum Dose	54.0(Gy)
Pituitary	Maximum Dose	54.0(Gy)
TM L	Maximum Dose	54.0(Gy)
TM R	Maximum Dose	54.0(Gy)
Inner Ears	Maximum Dose	54.0(Gy)
PAROTIDS	Maximum Volume of PAROTIDS covered by 50 Gy	30.0(%)
Esophagus	Mean Dose Uplimit	40.0(Gy)
Trachea	Mean Dose Uplimit	40.0(Gy)
Thyroid	Maximum Volume of Thyroid covered by 50Gy	50.0(%)
Mandible	Mean Dose Uplimit	50.0(Gy)
Oral Cavity	Mean Dose Uplimit	50.0(Gy)
Larynx	Mean Dose Uplimit	60.0(Gy)
Neck	Maximum Dose	40.0(Gy)